3D physics-based modelling of Ge-on-Si waveguide p-i-n photodetectors

Marco Vallone*, Andrea Palmieri*, Marco Calciati*, Francesco Bertazzi*†, Michele Goano*†, Giovanni Ghione*, Fabrizio Forghieri‡

* Dipartimento di Elettronica e Telecomunicazioni, Politecnico di Torino, corso Duca degli Abruzzi 24, 10129 Torino, Italy
† IEIIT-CNR, Politecnico di Torino, corso Duca degli Abruzzi 24, 10129 Torino, Italy
‡ CISCO Photonics, 20871 Vimercate (MB), Italy
E-mail: giovanni.ghione@polito.it, fforghie@cisco.com

***Abstract*—Considering a Ge-on-Si waveguide p-i-n photodetector structure inspired by the literature, we have investigated the role of the detector geometry on its electrical and optical (O/E) bandwidth. Due to the structural complexity of the detector, three-dimensional coupled optical and electrical simulations were needed to implement an accurate model. To make an extensive 3D optimization study possible with an acceptable computational effort, numerical simulations were complemented by simplified analytical models, which helped to identify the most promising regions in the device geometrical parameter space.**

The low-cost integration of optoelectronic components with Si-based electronic devices and circuits can be achieved today by *silicon photonics*, which exploits the compatibility of Si-based optoelectronic devices with current CMOS fabrication technologies (e.g., SOI) and the low cost compared to III-V-based optical interconnects [1]. Germanium-on-silicon (Ge-on-Si) near-infrared (NIR) photodetectors have been proposed in recent years as a key component of integrated silicon photonics platforms, using Si for optical guiding and Ge as NIR absorbing material [2], [3].

We have investigated a literature-inspired [4] Ge-on-Si p-i-n photodetector (Fig. 1), with the aims of assessing the role of its geometry on the electrical and optical bandwidth, and of identifying the modeling issues to be addressed. In the structure under study, a narrow Gaussian beam with wavelength $\lambda = 1310$ nm, launched in the input waveguide, widens when reaching a 15 μm long taper, then irradiates into a Ge absorber layer, $\approx$ 15 μm long and $\approx$ 4 μm wide, intrinsic apart from a thin, strongly p-doped layer below the bias contact. The silicon layer beneath the Ge absorber is moderately n-doped, to efficiently sweep out the photogenerated carriers. Silicon oxide, not shown in Fig. 1 for clarity, has been included in the simulated structure below the Si layer and all around Ge.

To investigate the complex behavior of this device, three-dimensional (3D) combined optical and electrical simulations were necessary [5]. We used a commercial numerical simulator [6] implementing both a drift-diffusion (DD) solver for carrier transport and the finite difference time domain method (FDTD) [7]–[9] to solve Maxwell's equations. Within this framework, it was crucial to fine-tune the optical grid, whose step was chosen around $\lambda/50$ in order to realistically describe the beam

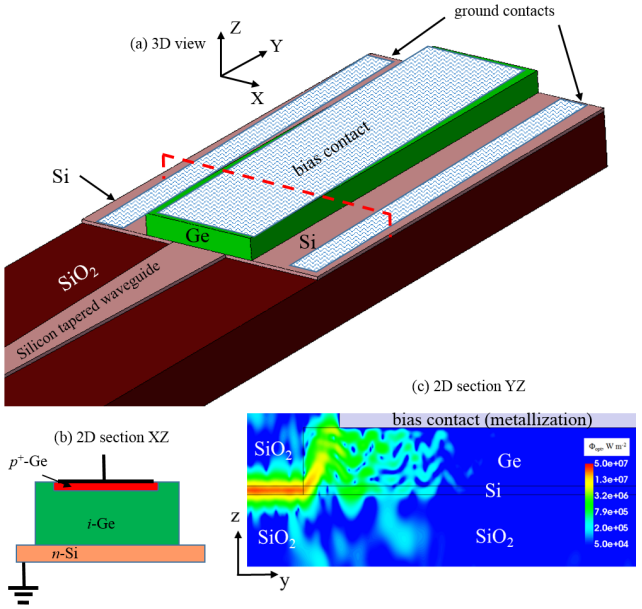

Fig. 1. Perspective view (a) and cross section (b) of the Ge-on-Si p-i-n detector under study. The light travelling in the tapered Si waveguide is irradiated into the Ge absorber (c).

adiabatical widening into the taper, avoiding spurious back-scattering and higher mode excitation. The computed optical field (Fig. 1(c)) enters as a source term in the DD equations describing the electrical problem, which were discretized with a mesh spacing between 5 nm and 0.1 μm in the detector region. The Si and Ge electrical, transport and absorption properties were treated as in [2], [10], also considering carrier velocity saturation in Ge [11], [12] with $v_{\mathrm{sat}} \approx 0.75 \times 10^7$ cm s^{-1}.

Fig. 2 shows the high nonuniformity of the electron velocity distribution in the Ge layer under illumination and reverse bias (-3 V), induced by screening from photogenerated carriers. This nonuniformity is an issue for simple analytical models trying to describe the detector as an RC circuit [13] and to calculate the electrical H_{el} and/or optical H_{opt} small-signal frequency response, which is determined by the numerical simulator by applying a small perturbation of the incident wave

978-1-5090-5323-0/17/$31.00 ©2017 IEEE

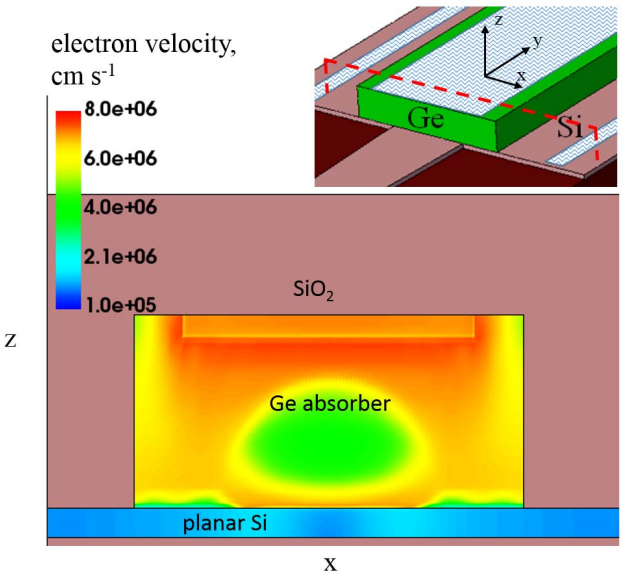

Fig. 2. Map of the electron velocity in the xz plane located at $y = 0.5\,\mu$m from the Ge absorber edge.

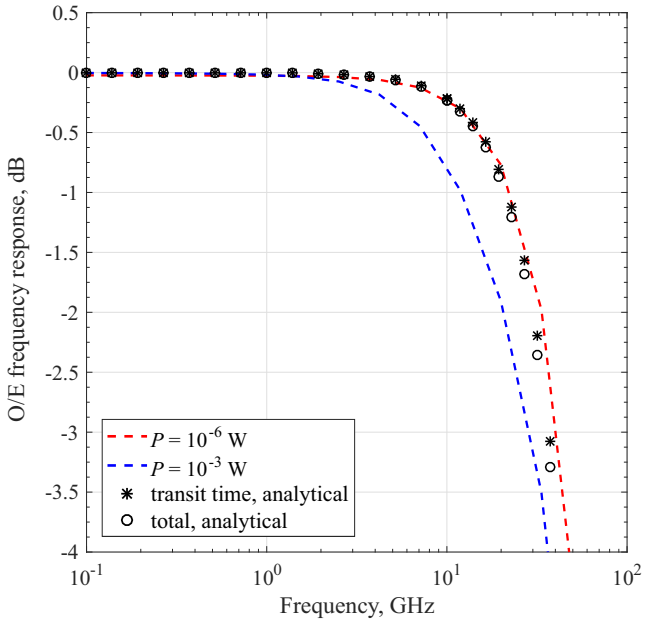

Fig. 3. Optical frequency response at a bias $V = -1.5\,$V, for two values of the optical power P coupled in the waveguide: the comparison between numerical and analytical model reveals that the device is transit-time limited.

power $\delta P_0 \exp(\mathrm{i}\omega t)$, where $\omega = 2\pi f$ and f is the small-signal light modulation frequency.

In order to check, validate and better understand the results of 3D numerical simulations, we developed an analytical model which treats the detector as a multi-section RC circuit, and allows to estimate the photodetector capacitance, its series resistance, and the responses H_{el} and H_{opt} (an example for H_{opt} is shown in Fig. 3). The model provides a fast approximation of the -3 dB cutoff frequency f_{3dB} as a function of the Ge layer length L and thickness d (Fig. 4), separating the transit-time contribution from all the others. With reference to Fig. 4, we see that transit-time effects are predicted to be dominant in the region above the parameter locus identified by the dashed line, while the bandwidth is dominated by RC effects below the same line; this suggests the need for a careful choice of the value of d, given a lenght L of the detector large enough to yield satisfactory responsivity. The results of the analytical model can be exploited to identify near-optimum regions in the geometrical parameter space, where CPU-intensive 3D simulation campaigns can be targeted in order to get more accurate results.

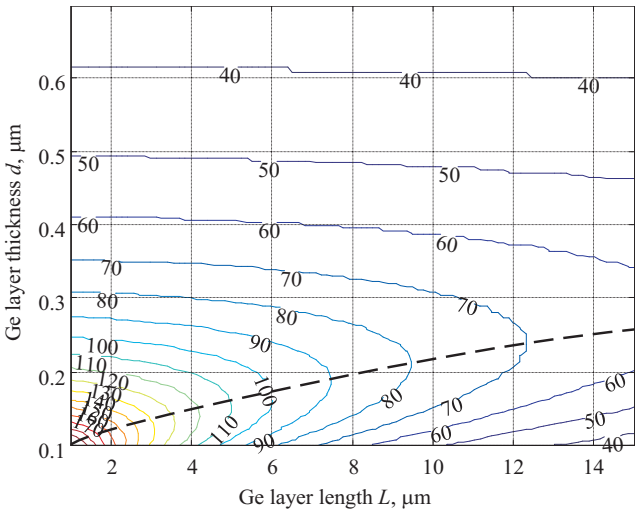

Fig. 4. Optical AC analysis with the analytical model: -3 dB cutoff frequency response at a bias $V = -3\,$V under illumination ($P = 2\,$mW).

Acknowledgments

This work was supported by CISCO Systems under a Sponsored Research Agreement Contract.

References

[1] R. Soref, *IEEE J. Select. Topics Quantum Electron.* **12**, 1678 (2006).
[2] S. J. Koester, J. D. Schaub, G. Dehlinger, J. O. Chu, *IEEE J. Select. Topics Quantum Electron.* **12**, 1489 (2006).
[3] Y. Ishikawa, S. Saito, *IEICE Electron. Express* **11**, 20142008 (2014).
[4] T. Yin, *et al.*, *Opt. Eng.* **15**, 13965 (2007).
[5] M. Vallone, *et al.*, *J. Electron. Mater.* **43**, 3070 (2014).
[6] Synopsys, Inc., Mountain View, CA, *Sentaurus Device User Guide. Version K-2015.06* (2015).
[7] K. Yee, *IEEE Trans. Antennas Propagation* **14**, 302 (1966).
[8] D. Vasileska, S. M. Goodnick, G. Klimeck, *Computational Electronics. Semiclassical and Quantum Device Modeling and Simulation* (CRC Press, Boca Raton, FL, 2010).
[9] M. Vallone, *et al.*, *J. Electron. Mater.* **45**, 4524 (2016).
[10] M. E. Levinshtein, S. L. Rumyantsev, M. S. Shur, eds., *Properties of Advanced Semiconductor Materials GaN, AlN, InN, BN, SiC, SiGe* (John Wiley & Sons, New York, 2001).
[11] C. Canali, G. Majni, R. Minder, G. Ottaviani, *IEEE Trans. Electron Devices* **22**, 1045 (1975).
[12] R. Quay, C. Moglestue, V. Palankovski, S. Selberherr, *Mater. Sci. Semicond. Processing* **3**, 149 (2000).
[13] Y. Ishikawa, K. Wada, *IEEE Photon. J.* **2**, 306 (2010).